Talanta 197 (2019) 431–435

Contents lists available at ScienceDirect

Talanta

journal homepage: www.elsevier.com/locate/talanta

Construction of a novel far-red fluorescence light-up probe for visualizing intracellular peroxynitrite

Wangbo Qu[a,1], Changhe Niu[c,1], Xiaoyu Zhang[a], Wei Chen[d], Fabiao Yu[b], Heng Liu[a,b,d,*], Xiuhua Zhang[a], Shengfu Wang[a]

[a] Hubei Collaborative Innovation Center for Advanced Organic Chemical Materials, Ministry of Education Key Laboratory for the Synthesis and Application of Organic Functional Molecules & College of Chemistry and Chemical Engineering, Hubei University, Wuhan 430062, PR China
[b] Institute of Functional Materials and Molecular Imaging, College of Clinical Medicine, Key Laboratory of Hainan Trauma and Disaster Rescue, College of Emergency and Trauma, Hainan Medical University, Haikou 571199, PR China
[c] Wuhan Children's Hospital, Tongji Medical College, Huazhong University of Science and Technology, Wuhan 430016, PR China
[d] Department of Chemistry, Washington State University, Pullman, WA 99164, United States

ARTICLE INFO

Keywords:
Dicyanomethylene benzopyran derivative
Naked-eyes detection
Far-red
Fluorescence off-on
Imaging endogenous peroxynitrite

ABSTRACT

Peroxynitrite ($ONOO^-$) is an important reactive oxygen species (ROS), which can react with a variety of biologically active species and cause many diseases, such as cancer, neurodegenerative disorders. Herein, we develop a novel far-red fluorescent probe DCM-KA, which is equipping with α-ketoamide moiety caged DCM-NH_2. The probe exhibits fluorescence off-on response to $ONOO^-$ over other biological interfering analytes by $ONOO^-$-induced α-ketoamide deprotection reaction. More importantly, the probe is biocompatible and has been successfully utilized to visualize endogenous $ONOO^-$ production in macrophage cell line J774A.1.

1. Introduction

Peroxynitrite ($ONOO^-$), a kind of extremely reactive oxygen species (ROS) produced through in vivo coupling reaction of nitric oxide (•NO) and superoxide radicals ($O_2^{\bullet-}$) with an average reaction rate constant of $10^{10}\ M^{-1}\ s^{-1}$, is included in the pathogenesis of various diseases [1–3]. Recent reports demonstrate that $ONOO^-$ can react with a wide array of biologically active species, such as enzymes, proteins, nucleic acids and lipids, thereby affecting cellular processes and even causing cell necrosis and apoptosis [4–7]. For example, $ONOO^-$ can nitrate biomolecules to alter cell signal transduction pathways, realizing modulation of the physiological processes of cells [8–10]. Imbalance of $ONOO^-$ has also been reported to be linked to an increasing list of diseases, including neurodegenerative disorders like Alzheimer's disease, cancer, circulatory shock and reperfusion injury [11–14]. Therefore, development of detection method for $ONOO^-$ is of great significance for deeper understanding its functions in complicated biological systems.

However, it is a huge challenge to detect $ONOO^-$ in physiological conditions in virtue of its short half-life (< 10 ms), low concentration and high reactivity [15]. Though a number of methods have been used for $ONOO^-$ detection, fluorescence imaging technology with fluorescent probes receive increasing attention due to easy operation, high sensitivity and selectivity and in-situ detection [16–19]. Of note, long-wavelength fluorophores with emission in far-red or near-infrared (NIR) region (λ_{em} > 600 nm) are commonly used for designing probes for bioimaging with rare autofluorescence interference, low photodamage and deeper tissue penetration [20].

So far, a variety of fluorescent probes have been reported for $ONOO^-$ detection based on different responsive sites, such as methyl(4-hydroxyphenyl)amino [21–25], boronic acid/boronates [26], hydrazide [27–30], organo-selenium/tellurium [31,32], trifluoromethyl ketone [33], α-ketoamide [34–36], double carbon bond [37–39] and others [40–42]. But fluorescent probes for $ONOO^-$ that can emit in far-red or NIR region with excellent performance are still rare. Herein, we described a simple far-red fluorescent probe DCM-KA for specific detection of $ONOO^-$ with a large Stokes Shift (up to 160 nm). This probe was constructed by mounting an α-ketoamide as a recognizing moiety onto the DCM-NH_2 core (Scheme 1a). As expected, the probe displayed very weak fluorescence because the electron-withdrawing α-ketoamide moiety attenuated intramolecular charge transfer (ICT) and photo-induced electron transfer (PET) effects. When $ONOO^-$ was present, α-ketoamide moiety was removed and released the fluorophore DCM-

* Corresponding author at: Hubei Collaborative Innovation Center for Advanced Organic Chemical Materials, Ministry of Education Key Laboratory for the Synthesis and Application of Organic Functional Molecules & College of Chemistry and Chemical Engineering, Hubei University, Wuhan 430062, PR China.
E-mail address: liuheng11b@hubu.edu.cn (H. Liu).
[1] These two authors contributed equally to this work (W.B. Qu and C.H. Niu).

https://doi.org/10.1016/j.talanta.2019.01.065
Received 7 November 2018; Received in revised form 4 January 2019; Accepted 16 January 2019
Available online 17 January 2019
0039-9140/

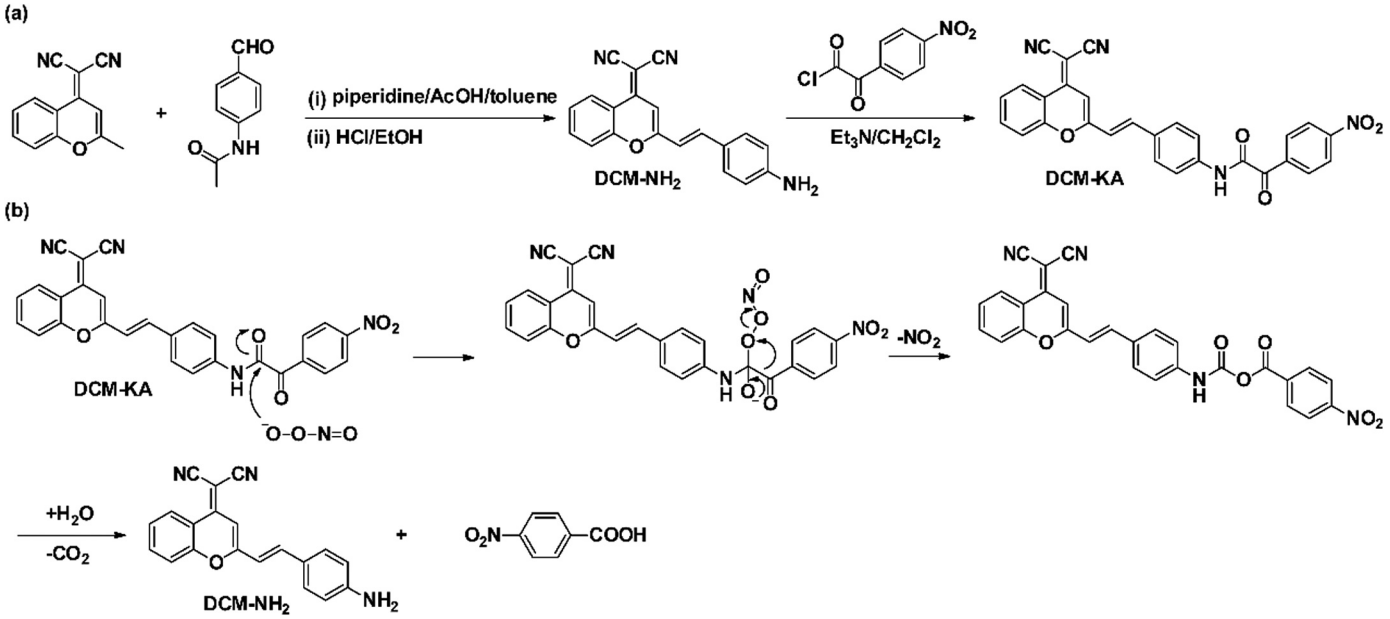

Scheme 1. (a) Synthetic route of DCM-KA. (b) Proposed sensing mechanism of DCM-KA toward $ONOO^-$.

NH_2, which resulted in restoring fluorescence. The probe also showed a rapid off-on response to $ONOO^-$ in 90 s with high selectivity and sensitivity. Furthermore, the probe was capable of imaging endogenous $ONOO^-$ in living macrophage cells.

2. Experimental section

2.1. Reagents and apparatus

Unless stated otherwise, all reagents and solvents for the experiments were purchased from commercial suppliers and used without further purification. ^1H NMR and ^{13}C NMR were performed on a BRUKER 400 MHz spectrometer. ESI mass spectra were conducted on a Bruker ESI-TOF. All solutions used in this work were prepared by Ultrapure water (18.2 M cm^{-1}). UV–vis absorption spectra were measured with an Agilent Technologies Cary 60. Fluorescence spectra were obtained on an Agilent Cary Eclipse fluorescence spectrophotometer. Confocal images of $ONOO^-$ in J774A.1 cells were carried out on Olympus FV1000 laser scanning confocal microscope.

2.2. General procedure for the spectra measurement

The stock solution of DCM-KA (10.0 mM) was prepared in DMSO. Stock solutions of various analytes were prepared in ultrapure water. The resulting solution was kept at room temperature and then the absorption or fluorescence spectra were measured. All of fluorescence spectra were performed at the excitation wavelength 480 nm with excitation silts of 5 nm and emission slits of 10 nm.

2.3. Cell culture and fluorescence imaging

J774A.1 cells were grown in DMEM supplemented with 10% (v/v) FBS, 100 U/ml of penicillin and 100 U/ml of streptomycin. The cells were incubated in a humidified incubator at 37 °C, 5% CO_2. The cytotoxicity of DCM-KA was evaluated by CCK-8 assay. J774A.1 cells were seeded on Petri dishes prior to CLSM imaging. For imaging endogenous production of $ONOO^-$ in J774A.1 cells, three series of fluorescence imaging experiments were carried out. Firstly, the cells were incubated with only DCM-KA (10 μM); secondly, the cells were treated with lipopolysaccharides (LPS 1 μg/ml) and interferon-γ (IFN-γ 100 ng/ml) for 10 h, and then incubated with phorbol 12-myristate 13-acetate (PMA 10 nM) for 0.5 h and DCM-KA (10 μM) for another 0.5 h; thirdly, as a control experiment, the cells incubated with LPS (1 μg/ml), IFN-γ (100 ng/ml), aminoguanidine (AG, an inhibitor of nitric oxide synthase, 1 mM) followed by the incubation with PMA for 0.5 h and DCM-KA (10 μM) for another 0.5 h. The cells were washed with PBS buffer for three times before subjecting to fluorescence imaging measurements with laser scanning confocal microscope. Emission was collected at red channel (600–700 nm) with 488 nm excitation.

2.4. Synthesis of DCM-NH_2

N-(4-formylphenyl)acetamide (163 mg, 1.0 mmol) was added to a solution of 2-(2-methyl-4H-chromen-4-ylidene) malononitrile (229 mg, 1.1 mmol), piperidine (0.15 ml) and acetic acid (0.15 ml) in toluene (10 ml). The resulting mixture was refluxed under argon for 5 h. For work up, the mixture was cooled to room temperature and filtered to give an orange solid, followed by addition of conc. HCl and EtOH (v/v 2/1, 30 ml). Then the mixture was refluxed for another 5 h. After the reaction was completed, the mixture was quenched with saturated $NaHCO_3$ (aq) and extracted with ethyl acetate. The organic layer was dried over Na_2SO_4 and concentrated in vacuo. Purification by flash column chromatography (eluent: DCM) to give the desired product DCM-NH_2 (124 mg, 40%). ^1H NMR (400 MHz, d_6-DMSO): δ 8.68 (d, J = 8.3 Hz, 1 H), 7.86 (t, J = 7.8 Hz, 1H), 7.72 (d, J = 8.4 Hz, 1H), 7.60 (d, J = 15.8 Hz, 1H), 7.55 (t, J = 8.3 Hz, 1H), 7.46 (d, J = 8.6 Hz, 2H), 7.04 (d, J = 15.7 Hz, 1H), 6.82 (s, 1H), 6.60 (d, J = 8.6 Hz, 2H), 6.02 (s, 2H); ^{13}C NMR (100 MHz, d_6-DMSO): δ 159.7, 152.5, 152.1, 152.0, 140.6, 135.0, 130.7, 125.9, 124.5, 122.3, 118.9, 117.8, 117.2, 116.4, 113.8, 112.4, 104.7, 57.4; ESI-MS: Calcd for $C_{20}H_{13}N_3O$ $[M+H]^+$ 311.1059 found 312.1137, $[M + Na]^+$ 334.0956 found 334.0962.

2.5. Synthesis of DCM-KA

Oxalyl chloride (225 μl, 2.64 mmol) was dropwise added to a solution of 2-(4-nitrophenyl)-2-oxoacetic acid (172 mg, 0.88 mmol) in dichloromethane (5 ml) at 0 °C. Then two drops of N, N-dimethylformamide was added and the resulting mixture was refluxed for 1 h. After evaporation of the solvent, a solution of DCM-NH_2 (70 mg, 0.22 mmol), triethylamine (123 μl, 0.88 mmol) in dichloromethane (5 ml) were added and the mixture was stirred for another 1 h. After evaporation of the solvent, the obtained mixture was purified by flash column

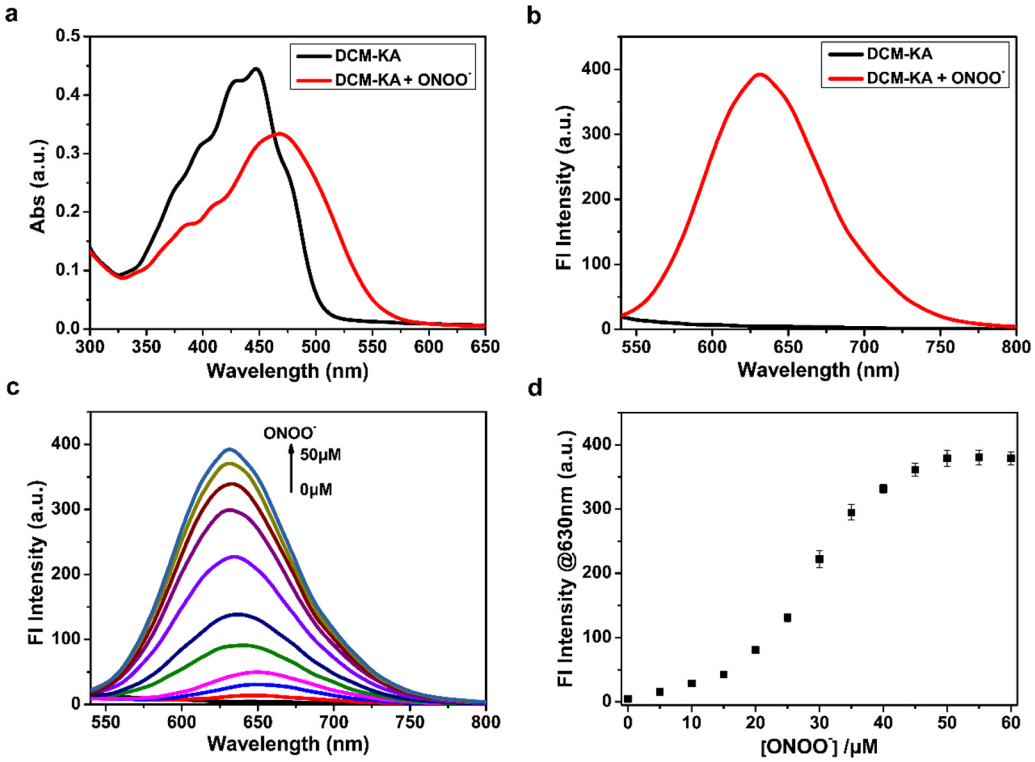

Fig. 1. (a) UV–vis absorption spectra of DCM-KA (10 μM) before and after addition of $ONOO^-$ (50 μM). (b) Fluorescence spectra of DCM-KA (10 μM) before and after addition of $ONOO^-$ (50 μM). (c) Fluorescence response of DCM-KA (10 μM) to $ONOO^-$ in the presence of various amounts (0–50 μM). (d) The relationship between the fluorescence intensities at 630 nm of DCM-KA and $ONOO^-$ concentrations (0–60 μM).

chromatography on silica gel (eluent: DCM) to give the desired product DCM-KA (46 mg, 42.8%). ^{1}H NMR (400 MHz, d_6-DMSO): δ 11.21 (s, 1H), 8.70 (d, J = 8.1 Hz, 1H), 8.40–8.31 (m, 4H), 7.93–7.78 (m, 6H), 7.69 (d, J = 15.9 Hz, 1H), 7.59 (t, J = 7.6 Hz, 1H), 7.42 (d, J = 16.0 Hz, 1H), 6.98 (s, 1H); ^{13}C NMR (100 MHz, d_6-DMSO): δ 187.2, 162.5, 158.2, 152.9, 152.0, 150.5, 139.4, 138.0, 137.6, 135.4, 131.7, 131.3, 129.1, 126.2, 124.6, 123.8, 120.5, 119.1, 118.9, 117.2, 117.1, 115.9, 106.6, 60.2; ESI-MS: Calcd for $C_{28}H_{16}N_4O_5$ $[M-H]^-$ 488.1121, found 487.1051.

3. Results and discussion

3.1. Spectra response of DCM-KA to $ONOO^-$

Photophysical properties of DCM-KA were carried out in 10 mM PBS buffer-THF solution (1:1, v/v, pH 7.4) at 25 ℃. As can be seen from Fig. 1a, DCM-KA had two major absorption peaks at around 429 nm and 447 nm. Upon the addition of $ONOO^-$ to the solution, the absorption wavelength red-shifted to 470 nm (Fig. S7). DCM-KA itself showed almost no fluorescence in the absence of $ONOO^-$; however, reaction with $ONOO^-$ triggered a noticeable fluorescence enhancement along with emission blue-shift from 650 nm to 630 nm (Fig. 1b). Surprisingly, the probe exhibited a large Stokes Shift (up to 160 nm), which was beneficial for eliminating self-quenching and produced a strong fluorescence signal in bioimaging. The dramatic changes in the absorption and fluorescence spectra might be attributed to structural variations of DCM-KA. To prove this assumption, ESI-MS analysis was conducted (Fig. S10). The mixture of DCM-KA and excess $ONOO^-$ showed the presence of peaks at m/z 310.0982 and 166.0142, which were ascribed to the releasing fluorophore DCM-NH_2 ($[M-H]^-$) and 4-nitrobenzoic acid ($[M-H]^-$). The results further confirmed the proposed sensing mechanism as shown in Scheme 1b.

Fig. 1c and Fig. 1d illustrated that a large fluorescence increase at 630 nm was obtained with the increasing amounts of $ONOO^-$ upon excitation with 480 nm, where the fluorescence intensities were linear with $ONOO^-$ concentrations in the range of 0–15 μM (linear equation: $y = 2.5047 \times + 4.5572$, $R^2 = 0.9983$) and 15–45 μM (linear equation: $y = 11.2358 \times - 129.9348$, $R^2 = 0.9853$) (Fig. S8, S9). The limit of detection for DCM-KA toward $ONOO^-$ was determined to be 0.38 μM and 78 nM (S/N = 3), respectively. The results revealed that DCM-KA was a highly sensitive off-on fluorescent probe for sensing of $ONOO^-$.

Subsequently, the reaction kinetics of DCM-KA toward $ONOO^-$ was investigated (Fig. 2a). Almost no fluorescence changes of DCM-KA were observed in presence of $ONOO^-$, which suggested that the probe's photostability was very excellent. When 50 μM of $ONOO^-$ was added to the solution, the intensity of the emitted fluorescence at 630 nm showed a mutation and reached a plateau during 90 s with 85-fold fluorescence enhancement. The rapid response to $ONOO^-$ further confirmed that DCM-KA was suitable for bioimaging $ONOO^-$. The effect of pH on the response of DCM-KA was also explored under different pH values. As demonstrated in Fig. 2b, the background fluorescence of DCM-KA was very low over a wide pH range of 3.0–11.0. After treating with $ONOO^-$, a significant increase in fluorescence intensity was observed within the pH 3.0–11.0 range, which indicated the probe could work well in biological system.

The response of DCM-KA for $ONOO^-$ over other biological potential interfering analytes was then evaluated. Treatment with common ions (K^+, Na^+, Fe^{2+}, AcO^-, CO_3^{2-}) and amino acids (Leu, Thr, Gly, Ser, Arg) caused negligible fluorescence changes in the fluorescence intensity at 630 nm (Fig. 2c). Only when $ONOO^-$ was added produced remarkable fluorescence signals. Most importantly, ROS (H_2O_2, ClO^-, •OH, BrO^-, $^1O_2$), RNS (NO_2^-, NO_3^-) and RSS (HS^-, GSH, Cys, Hcy), which might interfere with detecting $ONOO^-$, also failed to trigger a fluorescence response (Fig. 2d). Additionally, addition of $ONOO^-$ induced an apparent color changes from light yellow to orange (Fig. 2e). Under the condition of irradiation using 365 nm UV lamp, only adding of $ONOO^-$ showed red fluorescence while other interfering species were almost no fluorescence (Fig. 2f).

3.2. Cell imaging

To expand the application of probe DCM-KA for bioimaging, we then utilized DCM-KA for imaging endogenous $ONOO^-$ production in macrophage cell line J774A.1. Prior to live cell imaging, the

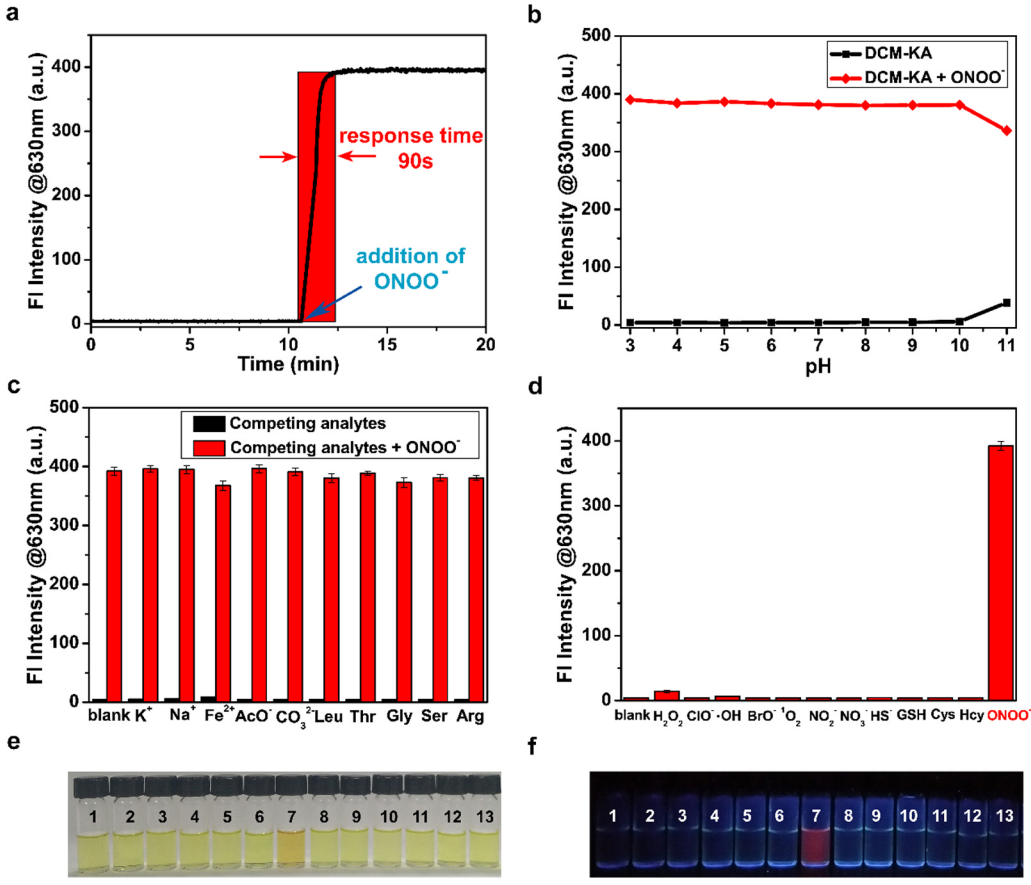

Fig. 2. (a) Time scan fluorometry of DCM-KA (10 μM) before and after treatment with of $ONOO^-$ (50 μM). (b) Fluorescence intensities at 630 nm of DCM-KA (10 μM) at different pH values in the absence and presence of $ONOO^-$ (50 μM). (c) Selectivity of DCM-KA (10 μM) toward various analytes. 300 μM for K^+, Na^+, Fe^{2+}, AcO^-, CO_3^{2-}, Leu, Thr, Gly, Ser and Arg. (d) Fluorescence responses of DCM-KA (10 μM) toward ROS, RNS and RSS species. 300 μM for H_2O_2、ClO^-、. OH、BrO^-、$^1O_2$、NO_2^-、NO_3^-、HS^-, 3 mM of GSH, 500 μM for Cys、Hcy. (e) Photographs of DCM-KA after the addition of various analytes under visible. (f) Photographs of DCM-KA after the addition of various analytes under UV irradiation of 365 nm. The photo of analytes: 1, blank; 2, H_2O_2; 3, ClO^-; 4,. OH; 5, BrO^-; 6, $^1O_2$; 7, $ONOO^-$; 8, NO_2^-; 9, NO_3^-; 10, HS^-; 11, GSH; 12, Cys; 13, Hcy.

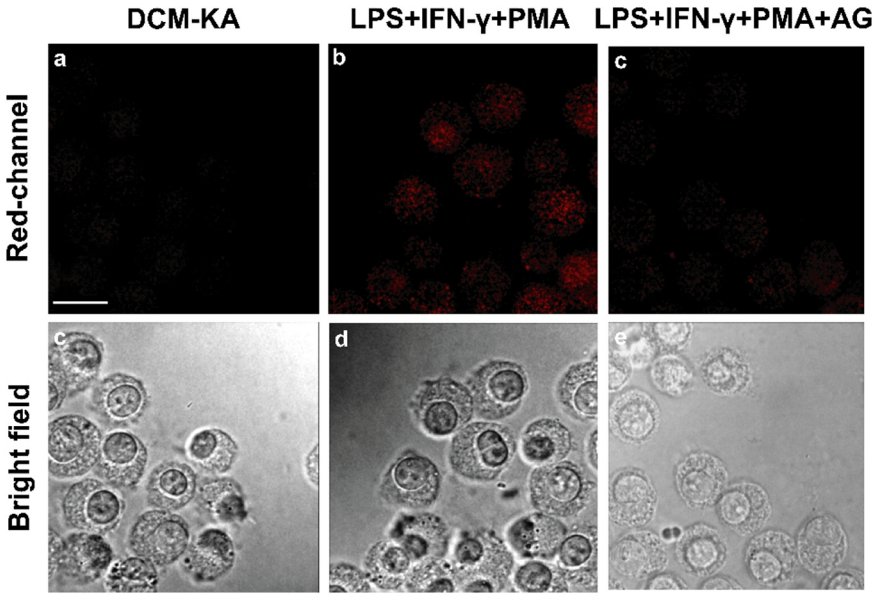

Fig. 3. Red channel (top row), bright field (down row) images of J774A.1 cells under different conditions. (a,c) Cells incubated with DCM-KA; (b, d) Cells were stimulated with LPS (1 μg/ml) and IFN-γ (100 ng/ml) for 10 h, and then incubated with PMA (10 nM) for 0.5 h and DCM-KA for another 0.5 h; (c, e) Cells were stimulated with LPS (1 μg/ml), IFN-γ (100 ng/ml) and AG (1 mM) for 10 h, and then incubated with PMA (10 nM) for 0.5 h and DCM-KA for another 0.5 h. Scale bar: 20 μm.

cytotoxicity of DCM-KA was first evaluated by CCK-8 assay and the results showed low cytotoxicity in the presence of different amounts of DCM-KA (Fig. S11), suggesting that DCM-KA was biocompatible and suitable for bioimaging. As demonstrated in Fig. 3, the cells only incubated with DCM-KA were almost non-fluorescent. When the cells were stimulated with lipopolysaccharides (LPS) and interferon-γ (IFN-γ), and then incubated with phorbol 12-myristate 13-acetate (PMA) and DCM-KA, strong fluorescence increases were observed. To confirm whether fluorescence signal changes of cells were due to the production of endogenous $ONOO^-$, the control experiment was carried out. The cells treated with LPS, IFN-γ, aminoguanidine (AG, an inhibitor of nitric oxide synthase) followed by the incubation with PMA and DCM-KA, much weak fluorescence signal was detected. These results demonstrated the great potential of probe DCM-KA for visualizing endogenous $ONOO^-$.

4. Conclusion

In summary, we reported a new type of far-red fluorescent probe DCM-KA, which selectively responded to $ONOO^-$ with a fluorescence off-on signal output. The probe not only showed a short response time (90 s), but also detected $ONOO^-$ in a wide pH range (3.0–11.0). In addition, treating with $ONOO^-$ would trigger color of the solution changed from light yellow to orange, enabling the probe to have the capacity to detect $ONOO^-$ by naked-eyes. Particularly, the probe could visualize endogenous $ONOO^-$ production in macrophage J774A.1 cells. This study provided a useful tool for understanding the effects of $ONOO^-$ in complex physiological systems.

Acknowledgement

This work was supported by the National Natural Science Foundation of China (NSFC.21602051), the Natural Science Foundation of Hubei Province (2016CFB200). H. Liu gratefully acknowledges the program of study abroad for young scholars by Education Department of Hubei.

Appendix A. Supporting information

Supplementary data associated with this article can be found in the online version at doi:10.1016/j.talanta.2019.01.065.

References

[1] G. Ferrer-Sueta, R. Radi, Chemical biology of peroxynitrite: kinetics, diffusion, and radicals, ACS. Chem. Biol. 4 (2009) 161–177.
[2] B. Halliwell, M. Whiteman, Measuring reactive species and oxidative damage in vivo and in cell culture: how should you do it and what do the results mean? Brit. J. Pharmacol. 142 (2004) 231–255.
[3] W.H. Koppenol, J.J. Moreno, W.A. Pryor, H. Ischiropoulos, J.S. Beckman, Peroxynitrite, a cloaked oxidant formed by nitric oxide and superoxide, Chem. Res. Toxicol. 5 (1992) 834–842.
[4] B. Alvarez, R. Radi, Peroxynitrite reactivity with amino acids and proteins, Amino. Acids. 25 (2003) 295–311.
[5] G. Ferrer-Sueta, N. Campolo, M. Trujillo, S. Bartesaghi, S. Carballal, N. Romero, B. Alvarez, R. Radi, Biochemistry of peroxynitrite and protein tyrosine nitration, Chem. Rev. 118 (2018) 1338–1408.
[6] R. Radi, Peroxynitrite, a stealthy biological oxidant, J. Biol. Chem. 288 (2013) 26464–26472.
[7] R. Radi, A. Cassina, R. Hodara, Nitric oxide and peroxynitrite interactions with mitochondria, Biol. Chem. 383 (2002) 401–409.
[8] L.O. Klotz, P. Schroeder, H. Sies, Peroxynitrite signaling: receptor tyrosine kinases and activation of stress-responsive pathways, Free Radic. Biol. Med. 33 (2002) 737–743.
[9] S. Levrand, B. Pesse, F. Feihl, B. Waeber, P. Pacher, J. Rolli, M.D. Schaller, L. Liaudet, Peroxynitrite is a potent inhibitor of NF-κB activation triggered by inflammatory stimuli in cardiac and endothelial cell lines, J. Biol. Chem. 280 (2005) 34878–34887.
[10] L. Liaudet, G. Vassalli, P. Pacher, Role of peroxynitrite in the redox regulation of cell signal transduction pathways, Front. Biosci. 14 (2009) 4809–4814.
[11] R. Ahmad, Z. Rasheed, H. Ahsan, Biochemical and cellular toxicology of peroxynitrite: implications in cell death and autoimmune phenomenon, Immunopharmacol. Immunotoxicol. 31 (2009) 388–396.
[12] P. Pacher, J.S. Beckman, L. Liaudet, Nitric oxide and peroxynitrite in health and disease, Physiol. Rev. 87 (2007) 315–424.
[13] C. Szabó, K. Módis, Pathophysiological roles of peroxynitrite in circulatory shock, Shock 34 (2010) 4–14.
[14] F. Torreilles, Sd Salman-Tabcheh, M.C. Guérin, J. Torreilles, Neurodegenerative disorders: the role of peroxynitrite, Brain. Res. Rev. 30 (1999) 153–163.
[15] R. Radi, Oxygen radicals, nitric oxide, and peroxynitrite: redox pathways in molecular medicine, Proc. Natl. Acad. Sci. USA 115 (2018) 5839–5848.
[16] F. Chen, J. Zhang, W. Qu, X. Zhong, H. Liu, J. Ren, H. He, X. Zhang, S. Wang, Development of a novel benzothiadiazole-based fluorescent turn-on probe for highly selective detection of glutathione over cysteine/homocysteine, Sens. Actuators. B. Chem. 266 (2018) 528–533.
[17] W. Chen, A. Pacheco, Y. Takano, J.J. Day, K. Hanaoka, M. Xian, A single fluorescent probe to visualize hydrogen sulfide and hydrogen polysulfides with different fluorescence signals, Angew. Chem. Int. Ed. 55 (2016) 9993–9996.
[18] S. Wang, L. Chen, P. Jangili, A. Sharma, W. Li, J.-T. Hou, C. Qin, J. Yoon, J.S. Kim, Design and applications of fluorescent detectors for peroxynitrite, Coord. Chem. Rev. 374 (2018) 36–54.
[19] D. Wu, A.C. Sedgwick, T. Gunnlaugsson, E.U. Akkaya, J. Yoon, T.D. James, Fluorescent chemosensors: the past, present and future, Chem. Soc. Rev. 46 (2017) 7105–7123.
[20] W. Chen, S. Xu, J.J. Day, D. Wang, M. Xian, A general strategy for development of near-infrared fluorescent probes for bioimaging, Angew. Chem. Int. Ed. 56 (2017) 16611–16615.
[21] T. Peng, X. Chen, L. Gao, T. Zhang, W. Wang, J. Shen, D. Yang, A rationally designed rhodamine-based fluorescent probe for molecular imaging of peroxynitrite in live cells and tissues, Chem. Sci. 7 (2016) 5407–5413.
[22] J. Park, C.H. Heo, H.M. Kim, J.I. Hong, Two-photon fluorescent probe for peroxynitrite, Tetrahedron. Lett. 57 (2016) 715–718.
[23] H. Zhang, J. Liu, Y.Q. Sun, Y. Huo, Y. Li, W. Liu, X. Wu, N. Zhu, Y. Shi, W. Guo, A mitochondria-targetable fluorescent probe for peroxynitrite: fast response and high selectivity, Chem. Commun. 51 (2015) 2721–2724.
[24] X. Li, R.R. Tao, L.J. Hong, J. Cheng, Q. Jiang, Y.M. Lu, M.H. Liao, W.F. Ye, N.N. Lu, F. Han, Y.Z. Hu, Y.H. Hu, Visualizing peroxynitrite fluxes in endothelial cells reveals the dynamic progression of brain vascular injury, J. Am. Chem. Soc. 137 (2015) 12296–12303.
[25] T. Peng, N.-K. Wong, X. Chen, Y.K. Chan, D.H.H. Ho, Z. Sun, J.J. Hu, J. Shen, H. El-Nezami, D. Yang, Molecular imaging of peroxynitrite with HKGreen-4 in live cells and tissues, J. Am. Chem. Soc. 136 (2014) 11728–11734.
[26] D. Lee, C.S. Lim, G. Ko, D. Kim, M.K. Cho, S.J. Nam, H.M. Kim, J. Yoon, A two-photon fluorescent probe for imaging endogenous $ONOO^-$ near nmda receptors in neuronal cells and hippocampal tissues, Anal. Chem. 90 (2018) 9347–9352.
[27] B. Zhu, M. Zhang, L. Wu, Z. Zhao, C. Liu, Z. Wang, Q. Duan, Y. Wang, P. Jia, A highly specific far-red fluorescent probe for imaging endogenous peroxynitrite in the mitochondria of living cells, Sens. Actuators. B Chem. 257 (2018) 436–441.
[28] D. Liu, S. Feng, G. Feng, A rapid responsive colorimetric and near-infrared fluorescent turn-on probe for imaging exogenous and endogenous peroxynitrite in living cells, Sens. Actuators. B Chem. 269 (2018) 15–21.
[29] D. Wu, J.C. Ryu, Y.W. Chung, D. Lee, J.H. Ryu, J.H. Yoon, J. Yoon, A far-red-emitting fluorescence probe for sensitive and selective detection of peroxynitrite in live cells and tissues, Anal. Chem. 89 (2017) 10924–10931.
[30] H. Li, X. Li, X. Wu, W. Shi, H. Ma, Observation of the generation of $ONOO^-$ in mitochondria under various stimuli with a sensitive fluorescence probe, Anal. Chem. 89 (2017) 5519–5525.
[31] F. Yu, P. Li, B. Wang, K. Han, Reversible near-infrared fluorescent probe introducing tellurium to mimetic glutathione peroxidase for monitoring the redox cycles between peroxynitrite and glutathione in vivo, J. Am. Chem. Soc. 135 (2013) 7674–7680.
[32] B. Wang, F. Yu, P. Li, X. Sun, K. Han, A BODIPY fluorescence probe modulated by selenoxide spirocyclization reaction for peroxynitrite detection and imaging in living cells, Dyes. Pigments. 96 (2013) 383–390.
[33] D. Yang, H.L. Wang, Z.N. Sun, N.W. Chung, J.G. Shen, A highly selective fluorescent probe for the detection and imaging of peroxynitrite in living cells, J. Am. Chem. Soc. 128 (2006) 6004–6005.
[34] J.B. Li, L. Chen, Q. Wang, H.W. Liu, X.X. Hu, L. Yuan, X.B. Zhang, A bioluminescent probe for imaging endogenous peroxynitrite in living cells and mice, Anal. Chem. 90 (2018) 4167–4173.
[35] Y. Li, X. Xie, X.E. Yang, M. Li, X. Jiao, Y. Sun, X. Wang, B. Tang, Two-photon fluorescent probe for revealing drug-induced hepatotoxicity via mapping fluctuation of peroxynitrite, Chem. Sci. 8 (2017) 4006–4011.
[36] D. Cheng, W. Xu, L. Yuan, X. Zhang, Investigation of drug-induced hepatotoxicity and its remediation pathway with reaction-based fluorescent probes, Anal. Chem. 89 (2017) 7693–7700.
[37] B. Guo, J. Jing, L. Nie, F. Xin, C. Gao, W. Yang, X. Zhang, A lysosome targetable versatile fluorescent probe for imaging viscosity and peroxynitrite with different fluorescence signals in living cells, J. Mater. Chem. B 6 (2018) 580–585.
[38] X. Jia, Q. Chen, Y. Yang, Y. Tang, R. Wang, Y. Xu, W. Zhu, X. Qian, FRET-based mito-specific fluorescent probe for ratiometric detection and imaging of endogenous peroxynitrite: dyad of Cy3 and Cy5, J. Am. Chem. Soc. 138 (2016) 10778–10781.
[39] X. Zhou, Y. Kwon, G. Kim, J.H. Ryu, J. Yoon, A ratiometric fluorescent probe based on a coumarin–hemicyanine scaffold for sensitive and selective detection of endogenous peroxynitrite, Biosens. Bioelectron. 64 (2015) 285–291.
[40] Z.H. Li, R. Liu, Z.L. Tan, L. He, Z.L. Lu, B. Gong, Aromatization of 9,10-dihydroacridine derivatives: discovering a highly selective and rapid-responding fluorescent probe for peroxynitrite, ACS Sens. 2 (2017) 501–505.
[41] D. Cheng, Y. Pan, L. Wang, Z. Zeng, L. Yuan, X. Zhang, Y.T. Chang, Selective visualization of the endogenous peroxynitrite in an inflamed mouse model by a mitochondria-targetable two-photon ratiometric fluorescent probe, J. Am. Chem. Soc. 139 (2017) 285–292.
[42] Q. Zhang, N. Zhang, Y.T. Long, X. Qian, Y. Yang, Understanding the selectivity of a multichannel fluorescent probe for peroxynitrite over hypochlorite, Bioconjugate. Chem. 27 (2016) 341–353.